Nuclear Spin Relaxation in Paramagnetic Systems: Electron Spin Relaxation Effects under Near-Redfield Limit Conditions and Beyond

Jozef Kowalewski,*,† Claudio Luchinat,*,‡ Tomas Nilsson,*,†,§ and Giacomo Parigi*,‡

Physical Chemistry, Arrhenius Laboratory, Stockholm University, SE−10691 Stockholm, Sweden, and CERM and Department of Agricultural Biotechnology, University of Florence, Via L. Sacconi, 6, I-50019 Sesto Fiorentino, Italy

Received: March 1, 2002; In Final Form: May 7, 2002

The analysis of experimental relaxometric profiles of paramagnetic complexes is usually performed using the Solomon−Bloembergen−Morgan (SBM) theory. The SBM theory is not valid for slowly rotating systems when the electronic levels are split at zero field, in which case a modified theory developed in Florence should be used. However, for many interesting systems, including Gd-based contrast agents for MRI, the electron spin relaxation is rather close to the Redfield limit, where none of these approaches is valid. In the present paper, the SBM theory and modified versions of the Florence model are compared against a general theory valid beyond the Redfield limit (the so-called slow-motion theory). Significant differences are found already for the cases where the electron spin relaxation is in a regime near the Redfield limit, but still within it. Indeed, the values of the parameters describing the electron spin relaxation are underestimated for the SBM theory relative to those used in calculating the slow-motion profiles. The present results are relevant for the interpretation of relaxometric profiles of paramagnetic complexes and proteins, and for the interpretation of the behavior of contrast agents used in MRI, and should be taken into account when planning the improvement of the relaxometric properties for the next generation of contrast agents based on theoretical predictions.

Introduction

Paramagnetic relaxation enhancement (PRE) can be a rich source for structural and dynamical information of transition-metal complexes.[1−3] The field dependence of the PRE is usually presented as nuclear magnetic relaxation dispersion (NMRD) profiles (sometimes called relaxometric profiles) where the spin−lattice (and/or the spin−spin relaxation) of solvent protons are measured at magnetic fields ranging typically from 0.01 to 800 MHz proton Larmor frequency. Relaxometric profiles of paramagnetic complexes are usually fitted with the Solomon−Bloembergen−Morgan (SBM) equations[4−6] to obtain information, possibly in conjunction with other techniques, on the rotational correlation time of the complex, on the distance between metal and coordinated solvent molecule(s) (e.g., water), on the residence time of the coordinated solvent molecule(s), and on the electron spin relaxation time. Electron spin relaxation for $S \geq 1$ complexes in solution is usually described by a mechanism where the transient zero-field splitting (ZFS) interaction is modulated, because of instantaneous distortions of the coordination polyhedron induced by collision with solvent water molecules. The ZFS interaction is caused by second-order effects of the spin−orbit coupling in systems of $S \geq 1$. Theoretical approaches that take into account the presence of static ZFS, which is present in complexes of lower symmetry than O_h, are also available.[7−10]

The most important application of relaxometry is probably in the development of contrast agents[11−20] for magnetic resonance imaging (MRI). In fact, a full understanding of the relaxation properties of paramagnetic complexes is necessary for the development of criteria to guide synthetic chemists to make new compounds with improved relaxivity (PRE per unit concentration). Higher relaxivity implies lower doses in clinical applications and, therefore, lower toxicity. The relaxometric technique is also applied to many biologically relevant systems. Metalloproteins, for instance, have been extensively studied.[3,21−24] Direct information about the electron spin system through EPR measurements may, in fact, not be possible if the electron spin relaxation is very rapid, because the line shape is too broad (often the case for Ni(II)). However, Merbach and co-workers succeeded in combining NMRD profiles of Gd(III) complexes with EPR and ^{17}O relaxation measurements[15,17,25,26] and analyzed the data within the framework of a simple SBM approach.

The range of validity of the SBM equations and of the above-mentioned programs is limited by the common requirement: (i) the electron−lattice interaction energy, whose modulation is responsible for the spin relaxation, is smaller than the inverse of the correlation time, τ_v, for the modulation of the coupling itself, times $\hbar$ (Redfield limit). The approaches allowing for the static ZFS require, in addition, that (ii) the rotation of the whole complex (or tumbling motion) is slow relative the electron spin relaxation. Moreover, the SBM theory and the original version of the Florence model[7] assume that the presence of static ZFS does not affect largely the electron spin relaxation time due to modulation of transient ZFS. This point has already been analyzed and solved for $S = 1$ by Bertini et al.[9] and for $S \geq 1$ by the group in Stockholm.[10] In the following, we will refer to both these approaches as the modified Florence model because

* To whom correspondence should be addressed. Phone: +39 055 4574262. Fax: +39 055 4574253. E-mail: luchinat@cerm.unifi.it. E-mail: jk@tom.fos.su.se. E-mail: tomas@tom.fos.su.se. E-mail: parigi@cerm.unifi.it.

† Stockholm University.

‡ University of Florence.

§ Present address: Department of Biophysical Chemistry, Lund University, SE-22000 Lund, Sweden.

10.1021/jp020608p CCC: $22.00
Published on Web 07/20/2002

TABLE 1: Best-Fit of Relaxometric Data of Some Gd-Contrast Agents to Solomon−Bloembergen−Morgan Equations

complexes	$\tau_M\ 10^{-6}$ s	$\tau_r\ 10^{-12}$ s	$\tau_v\ 10^{-12}$ s	$\tau_{S0}\ 10^{-12}$ s	Δ_t cm^{-1}	r Å	ref
DTPA-Gd	0.30	58−73	18−25	82−95	0.034−0.037	3.1	11, 12, 15
BOPTA-Gd	0.20	88	26	76	0.034	3.0	12
DTPA-BMEA-Gd	0.39	93	20	87	0.037	3.1	15
DTPA-EOB−Gd	0.20	84	25	78	0.035	2.9	13
DPTA-SA-Gd	0.50	64	17	78	0.042	3.1	19
DTPA-B(etH)A-Gd	2.4	150	18	107	0.035	3.0	18

both of the corresponding computer programs are based on the original Florence NMRD program. In this work, we investigate the SBM theory and the modified Florence model and how their profiles and fitting parameters are affected by approaching the Redfield limit. In fact, the validity of the Redfield limit is questioned for many cases of interest,[27,28] in particular for Gd complexes commonly used and investigated for clinical use as contrast agents for MRI.

When the electron spin dynamics is outside the Redfield limit, a simple exponential process may not be sufficient to describe the electron spin relaxation and, in fact, explicit electron spin relaxation times (longitudinal or transverse) may therefore not be possible to define. This problem was theoretically solved by treating the electron spin and the lattice to which it is so strongly coupled as a composite lattice, using the Liouville superoperator formalism.[29−31] The nuclear spin is coupled to this generalized lattice containing both the electron spin and the classical degrees of freedom. No electron spin relaxation time or nucleus−lattice correlation time is defined. Two motions of the generalized lattice are considered: the complex rotation and the distortion of the coordination sphere. The latter motion is denoted as "pseudorotation". Both motions are described by the rotational diffusion equation, with different diffusion coefficients or correlation times. This approach is valid for arbitrary magnetic field, for arbitrary electron spin relaxation (i.e., both within the Redfield limit and in the slow motion regime), for arbitrary regime of the rotational motion, and, in general, for arbitrary values of the parameters included in the model. In this paper, we compare the simplified models against this general approach (the slow-motion theory). The name "slow-motion" originates from the situation when the motion modulating the relevant interaction that leads to relaxation is on the same time scale as the relaxation itself. This is equivalent to stating that the mean interaction strength of the interaction Liouvillian may be larger than, or at least comparable to, the inverse of the correlation time τ_v, which corresponds to the motion modulating the interaction.

Methods and Theory

In the SBM approach, a field dependent electron spin relaxation is described by the Bloembergen−Morgan equation[6,32]

$$R_{1e} = \frac{2\Delta_t^2}{50}[4S(S+1)-3]\left(\frac{\tau_v}{1+\omega_s^2\tau_v^2}+\frac{4\tau_v}{1+4\omega_s^2\tau_v^2}\right) \quad (1)$$

where Δ_t^2 is the mean squared fluctuation of the ZFS and τ_v is the correlation time for the instantaneous distortions of the metal coordination polyhedron. It must be pointed out that such an equation has been derived in the absence of a static ZFS term in the electron-spin Hamiltonian, which means that it has been derived assuming high-field conditions (i.e., the magnitude of the Zeeman interaction is much larger than static ZFS). Moreover, it represents an "average" electron spin relaxation time for the various nondegenerate transitions. An equation different from the SBM equations for R_{2e} is sometimes used to take into account this effect.[15] However, this effect is usually very small at low magnetic fields,[15] and thus, the fitting parameters remain virtually the same.

The Redfield limit (or motional narrowing condition) can be expressed by the relationship[3]

$$\Delta_t\tau_v \ll 1 \quad (2)$$

Therefore, in the Redfield limit, $\Delta_t^2\tau_v \ll \tau_v^{-1}$, and thus, at low magnetic fields

$$R_{1e} = \frac{2\Delta_t^2}{50}[4S(S+1)-3]\left(\frac{\tau_v}{1+\omega_s^2\tau_v^2}+\frac{4\tau_v}{1+4\omega_s^2\tau_v^2}\right) \ll \tau_v^{-1} \quad (3)$$

Because R_{1e} decreases with increasing field (as ω_s increases), R_{1e} is thus much smaller than τ_v^{-1} at all fields; that is, the relaxation time T_{1e} ($=R_{1e}^{-1}$) arising from the interaction can never be as short as the correlation time with which the interaction is modulated.

NMRD profiles for Gd-based contrast agents for MRI are usually fitted with the SBM equations,[11−15,17−20] which provide the best-fit parameter values, reported for some examples in Table 1. It can be seen, for instance for Gd-DTPA, that the electron spin relaxation time at low fields, τ_{s0}, is of the same order as τ_v. This means that the electron spin relaxation is really close to the Redfield limit.

Relaxometric profiles for various illustrative parameter sets (within and beyond the Redfield limit) have been calculated by using the general slow-motion theory for the $S = {}^7/_2$ and $S = 1$ systems. The former system is pertinent to gadolinium(III) complexes and the latter to nickel(II) complexes. The validity of using Redfield approaches was investigated by fitting the simplified models (i.e., SBM theory and the modified Florence model) to the slow-motion profiles. Used programs are described in refs 7, 9, 10, and 29−31.

Results

Gd-Based Contrast Agent Profiles. The relaxation rates as a function of the magnetic field were calculated with the slow-motion theory by setting values for the parameters close to those of a typical Gd-contrast agent. Thus, the profiles were calculated for $S = {}^7/_2$, $\tau_v = 20$ ps, and $\Delta_t = 0.05$ cm$^{-1} \equiv 9.42 \times 10^9$ s^{-1}. In this way, the product $\Delta_t\tau_v$ is equal to 0.19, slightly larger to that obtained for Gd-DTPA. Two protons in fast exchange (i.e., with $\tau_M \ll T_{1M}$, where τ_M is the exchange lifetime and T_{1M} is the nuclear spin relaxation time at the paramagnetic site) were assumed to be at 3 Å from the paramagnetic center. The rotational correlation time τ_r was taken to be 20, 60, 200, 600, and 2000 ps, to simulate different possible sizes of the molecule bearing the Gd ion. Calculations were performed both by assuming the absence of static ZFS and the presence of an axially symmetric static ZFS term, with $D = 0.12247$ cm^{-1}.

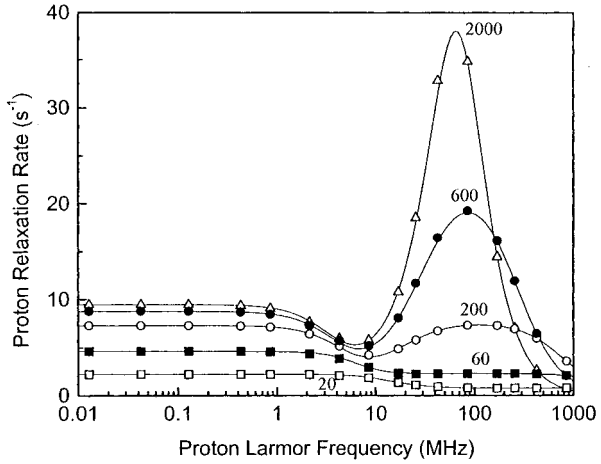

Figure 1. NMRD profiles calculated with the slow-motion theory ($\tau_r = 20 \times 10^{-12}$ s, □; 60×10^{-12} s, ■; 200×10^{-12} s, ○; 600×10^{-12} s, ●; 2000×10^{-12} s, △) for $S = {}^7/_2$ systems, two protons at 3.0 Å and $\Delta_t = 0.05$ cm^{-1}, $\tau_v = 20 \cdot 10^{-12}$ s and best fits (solid lines) performed using the SBM equations of the profiles calculated with the slow-motion theory. The profiles are labeled with the value of τ_r in picoseconds.

TABLE 2: Best-Fit Parameters Obtained Fitting the SBM Equations to the Slow-Motion Profiles Calculated without or with Static ZFS[a]

value used in the slow-motion calculation	best fit parameters for $D = 0$	best fit parameters for $D = 0.12247$ cm^{-1}
$\tau_r = 20$ ps	$\Delta_t = 0.029$ cm^{-1}	$\Delta_t = 0.029$ cm^{-1}
	$\tau_r = 20.1$ ps	$\tau_r = 20.0$ ps
	$\tau_v = 22.7$ ps	$\tau_v = 20.0$ ps
$\tau_r = 60$ ps	$\Delta_t = 0.036$ cm^{-1}	$\Delta_t = 0.022$ cm^{-1}
	$\tau_r = 60.1$ ps	$\tau_r = 60.0$ ps
	$\tau_v = 20.1$ ps	$\tau_v = 36.0$ ps
$\tau_r = 200$ ps	$\Delta_t = 0.044$ cm^{-1}	$\Delta_t = 0.042$ cm^{-1}
	$\tau_r = 200$ ps	$\tau_r = 200$ ps
	$\tau_v = 14.9$ ps	$\tau_v = 8.88$ ps
$\tau_r = 600$ ps	$\Delta_t = 0.045$ cm^{-1}	$\Delta_t = 0.039$ cm^{-1}
	$\tau_r = 598$ ps	$\tau_r = 599$ ps
	$\tau_v = 15.0$ ps	$\tau_v = 9.6$ ps
$\tau_r = 2000$ ps	$\Delta_t = 0.045$ cm^{-1}	$\Delta_t = 0.039$ cm^{-1}
	$\tau_r = 2000$ ps	$\tau_r = 2000$ ps
	$\tau_v = 15.4$ ps	$\tau_v = 9.2$ ps

[a] Parameters in the slow-motion theory: $S = {}^7/_2$, 2 protons at $r = 300$ pm, $\tau_v = 20$ ps, $\Delta_t = 0.05$ cm^{-1}, and $D = 0$ or 0.12247 cm^{-1}.

In Figure 1, we show the slow-motion data (symbols) for the case of $D = 0$ and the fitted profiles using the SBM equations (solid lines) for which Δ_t, τ_v, and τ_r were free to change. It is always possible to obtain a good fit, and the resulting best-fit parameters are reported in Table 2. The values indicate that τ_r is always well-determined, whereas the fitted Δ_t and τ_v are often significantly smaller than the values used in calculating the slow-motion profiles. This means that a non-negligible difference is caused by the closeness of the Redfield limit. In particular, τ_v is much smaller than the correct value for large molecules or complex adducts (25% smaller), and Δ_t is much smaller for small complexes (40% smaller). It can be noted that the best-fit values of Δ_t and τ_v, for τ_r equal to 60 ps, are those experimentally found by fitting the NMRD profiles of Gd-DTPA like complexes with the SBM equations.

In Figure 1, the low-field plateau of the slow-motion profiles is reduced as τ_r decreases (the complex becomes smaller) and one dispersion (the ω_S dispersion), present in the region around 10 MHz, moves toward higher frequencies with decreasing value of τ_r, as the nuclear correlation time decreases. In fact, the latter is given by the smallest of T_{1e} and τ_r. As soon as T_{1e} contributes to the nuclear correlation time, a peak appears in the high-field region, due to the combined effect of the field dependence of the electron spin relaxation (as shown by eq 1) and of the ω_I dispersion.

A special feature of the slow-motion theory, absent in the other approaches, is that the rotation is allowed to contribute to the electron spin relaxation. This can be expected to be most important for fast rotating systems [33] but does not seem to be a significant problem here, as indicated by the well-determined τ_r values.

Because of the large number of parameters affecting proton relaxation, and thus to be determined, it has been proposed that experimental NMRD profiles can be profitably analyzed in conjunction with data obtained with other experimental techniques, like ESR line shape analysis.[26,34,35] In this way, it should be possible to shrink the range of parameter (Δ_t and τ_v) values, as they have to be consistent with all techniques. However, all of the parameters extracted from ESR studies till now have been used in analyses performed within the validity of the Redfield limit (and thus the relevant equations are not correct near the Redfield limit), with the exception of one work by Merbach's group, recently published,[36] on the gadolinium(III) aqua ion. In the latter work, the simultaneous analysis of ^{17}O, ^{1}H, and EPR data has been extended beyond the electronic Redfield limit using Monte Carlo simulations.

Gadolinium(III) complexes often exhibit static ZFS interaction, and it is thus even more interesting to investigate whether the closeness of the Redfield limit can show similar features in this case as in the discussion of Figure 1. The profiles calculated with the slow-motion theory were fitted with the SBM equations, and the obtained best-fit values of the parameters Δ_t and τ_v are still significantly smaller than the correct ones (see Table 2). Moreover, the quality of the fit is not good. In fact, the SBM profiles (not shown) do not have the correct shape and the first dispersion comes at too low frequency. We return to this point in the Discussion section.

Because the modified Florence model is strictly valid only for slowly rotating systems, it cannot correctly be applied to rationalize these data. In the case of slow rotation, good agreement between the slow-motion theory and the modified Florence model is obtained if the electron spin relaxation clearly is within the Redfield limit, on account of the results in the earlier paper.[10]

Gd-Containing Macromolecule Profiles. To further elucidate the observations in Figure 1, we decided to make a set of slow-motion calculations ranging from within the Redfield limit and beyond it, for the case of slowly rotating systems of $S = {}^7/_2$ (e.g., Gd-containing macromolecules) with and without static ZFS present. The calculated slow-motion profiles for $D = 0$ were obtained with the following parameter values: $S = {}^7/_2$, $\tau_r = 10^{-6}$ s (so large that its effects become negligible), $\Delta_t = 0.05$ cm^{-1}, and τ_v from 1 to 100 ps. τ_v values of 100 ps are higher than any literature value, the latter being usually in the range of 2−50 ps[17] (τ_v can be overestimated due to the deficiencies of the pseudorotational model). However, high values of τ_v will bring the electron spin relaxation beyond the Redfield limit, which is what we want to simulate. Two protons in the fast exchange were assumed to be at 3.0 Å from the paramagnetic center.

Figure 2 shows the fit of the slow-motion profiles (symbols) with the SBM equations (solid lines) for the case of $D = 0$, and the best-fit parameters (Δ_t and τ_v) are reported in Table 3. The results show that the best-fit Δ_t and τ_v values are correct for $\Delta_t \tau_v = 0.01$ and 0.05. This means that the system is well

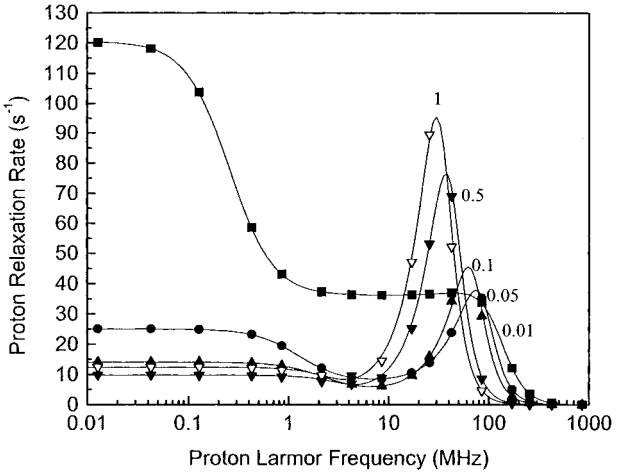

Figure 2. Proton relaxation rates calculated with the slow-motion theory ($\tau_v = 10^{-12}$ s, ■; 5×10^{-12} s, ●; 10^{-11} s, ▲; 5×10^{-11} s, ▼; 10^{-10} s, ▽) for $S = {}^7/_2$ systems, two protons at 3.0 Å and $\Delta_t = 0.05$ cm^{-1}, $\tau_r = 10^{-6}$ s and best fits (solid lines) performed using the SBM equations of the profiles calculated with the slow-motion theory. The profiles are labeled with the value of $\Delta_t\tau_v$.

within the Redfield limit, and no correction is needed. For $\Delta_t\tau_v \geq 0.1$, the best-fit Δ_t and τ_v values are significantly smaller. These results further support the observation in Figure 1 that the differences are due to the near-Redfield limit conditions.

The calculated slow-motion profiles with static ZFS present were performed using the same parameter values as for Figure 2, except for D that has the value 0.1 cm^{-1}. Figure 3 shows the fit of the slow-motion profiles (symbols) with the modified Florence NMRD program (solid lines), with the best-fit parameters (D, Δ_t, and τ_v) reported in Table 3.

The results of the modified Florence NMRD program show very good agreement for all parameters in the cases of $\Delta_t\tau_v \leq 0.1$. For larger values of $\Delta_t\tau_v$, the obtained parameter values of Δ_t and τ_v are, surprisingly, still in very good agreement with the values used in the slow-motion calculations. The obtained values of D in these latter cases are, however, slightly underestimated. These results indicate that the transition-frequency dependence in the electron spin relaxation changes as we move toward the Redfield limit and, in addition, that the presence of the static ZFS dominates the transition-frequency dependence in the electron spin relaxation even for near-Redfield limit conditions. For $\Delta_t\tau_v = 0.5$ and 1, a new feature can be noted in Figures 2−3: the relaxivity of the low-field plateau calculated using the slow-motion theory and the modified Florence NMRD program increases by increasing the value of τ_v, whereas it decreases in the profiles calculated with the SBM. This feature is also related to the transition-frequency dependence in the electron spin relaxation (vide infra).

Moreover, we tried also here to fit with the SBM equations. The produced profiles are very poor (not shown), and the obtained parameter values are clearly underestimated.

Ni-Containing Macromolecule Profiles. The same features as observed for $S = {}^7/_2$ in Figures 1−3 are expected to occur for $S = 1$ systems as well. In such systems, $\Delta_t\tau_v$ can be much larger than unity.[37] We want to investigate how the best-fit parameters are affected. The relaxometric profiles, calculated with the slow-motion theory, are displayed in Figure 4 (symbols) for a Δ_t value of 1 cm^{-1} and for different values of the correlation time τ_v that is responsible for electron spin relaxation (10^{-13}, 3×10^{-13}, 10^{-12}, 3×10^{-12}, 10^{-11}, 3×10^{-11}, 10^{-10}, and 3×10^{-10} s). These values of τ_v are chosen in order for the electron spin relaxation to be within the Redfield limit for some values and in the slow-motion regime for some others. Two fast exchanging protons were assumed to be at 3.0 Å from the paramagnetic center, and the rotational correlation time was set to 10^{-6} s (i.e., long enough so that the correlation time for nuclear spin relaxation is the electron spin relaxation time under any condition). The presence of an axially symmetric static ZFS, with $D = 1.2247$ cm^{-1}, is also assumed.

The profiles calculated with the slow-motion theory were fitted with the SBM theory and with the modified Florence NMRD program,[9] by leaving D, Δ_t, and τ_v free to change. The fitted profiles obtained using the SBM theory (not shown) are always in poor agreement with the slow-motion profiles. In the Redfield limit, the fitting of the SBM theory is indeed not possible, because of the presence of static ZFS. On the contrary, the fitted profiles of the modified Florence model, shown as solid lines in Figure 4, reproduce very well the slow-motion profiles within the Redfield limit (also shown earlier[9]). All best-fit parameters are reported in Table 4.

By approaching and passing the Redfield limit, the profiles calculated with the modified Florence NMRD program are not really sensitive to the value of the static ZFS D parameter, and good fits are obtained, even though with much smaller values of Δ_t and τ_v (up to 1 order of magnitude). This is somewhat different from what we found for $S = {}^7/_2$, where instead Δ_t did not change appreciably and D was obtained smaller. However, the sensitivity of τ_v is indeed similar to what we found for $S = {}^7/_2$ in the same motional regime.

In general, the static ZFS does not influence the electron spin relaxation (within the Redfield limit and for slowly rotating systems) for $S = 1$ to the same extent as for $S = {}^7/_2$, which has been discussed in an earlier paper by Nilsson and Kowalewski.[38] This would explain the insensitivity of the D parameter as we move toward the Redfield limit. The same behavior for the τ_v dependence as for $S = {}^7/_2$ in the previous section is, however, observed also in Figure 4 (i.e. the relaxivity increases as τ_v increases for the slow-motion profiles in the cases of $\Delta_t\tau_v \geq 1.9$).

Discussion

The physical picture of the features observed in Figures 1−4 is explained in this section with the aid of calculated profiles (i.e., no fitting) for the slow-motion theory, the SBM theory, and the modified Florence model. The calculations were performed for three cases of $S = {}^7/_2$ systems in the presence of static ZFS: (i) clearly within the Redfield limit ($\Delta_t\tau_v = 0.01$), (ii) near the Redfield limit ($\Delta_t\tau_v = 0.1$), and (iii) beyond the Redfield limit ($\Delta_t\tau_v = 1$). All parameter values are the same as in the corresponding cases of Figure 3.

The calculated profiles are shown in Figure 5 using the slow-motion theory (symbols), the modified Florence model (solid lines), and the SBM theory (dotted lines). Within the Redfield limit, the profile of the modified Florence model is in good agreement with that of the slow-motion theory, whereas some deviation in the low-field region is observed for the other two cases near and out of the Redfield limit. The SBM theory, on the other hand, shows good agreement only in the high-field part (above 30 MHz), whereas in the low-field region, there are significant differences for all three cases. Because the SBM theory is a high-field theory, this is not unexpected. In particular, the shape of the SBM profiles is very different than for the other approaches. In addition, the relaxivity in the low-field plateau calculated with the slow-motion theory or the modified Florence model is several times larger than the value calculated with the SBM equations.

TABLE 3: Best-Fit Parameters Obtained by Fitting the SBM Equations and the Modified Florence NMRD Program to the Slow-Motion Profiles Calculated with or without Static ZFS[a]

	values used in the slow-motion calculation $D = 0$, 0.1 cm^{-1}	best fit parameters for $D = 0$	best fit parameters from the SBM equations for $D = 0.1$ cm^{-1}	best fit parameters from the modified Florence NMRD program for $D = 0.1$ cm^{-1}
$\Delta_t\tau_v = 0.01$				$D = 0.107$ cm^{-1}
	$\Delta_t = 0.05$ cm^{-1}	$\Delta_t = 0.05$ cm^{-1}	$\Delta_t = 0.053$ cm^{-1}	$\Delta_t = 0.048$ cm^{-1}
	$\tau_v = 10^{-12}$ s	$\tau_v = 0.99 \cdot 10^{-12}$ s	$\tau_v = 1.2 \cdot 10^{-12}$ s	$\tau_v = 1.05 \cdot 10^{-12}$ s
$\Delta_t\tau_v = 0.05$				$D = 0.109$ cm^{-1}
	$\Delta_t = 0.05$ cm^{-1}	$\Delta_t = 0.049$ cm^{-1}	$\Delta_t = 0.051$ cm^{-1}	$\Delta_t = 0.049$ cm^{-1}
	$\tau_v = 5 \cdot 10^{-12}$ s	$\tau_v = 5 \cdot 10^{-12}$ s	$\tau_v = 5.4 \cdot 10^{-12}$ s	$\tau_v = 5.5 \cdot 10^{-12}$ s
$\Delta_t\tau_v = 0.1$				$D = 0.101$ cm^{-1}
	$\Delta_t = 0.05$ cm^{-1}	$\Delta_t = 0.048$ cm^{-1}	$\Delta_t = 0.046$ cm^{-1}	$\Delta_t = 0.050$ cm^{-1}
	$\tau_v = 10^{-11}$ s	$\tau_v = 0.93 \cdot 10^{-11}$ s	$\tau_v = 0.91 \cdot 10^{-11}$ s	$\tau_v = 1.1 \cdot 10^{-11}$ s
$\Delta_t\tau_v = 0.5$				$D = 0.086$ cm^{-1}
	$\Delta_t = 0.05$ cm^{-1}	$\Delta_t = 0.035$ cm^{-1}	$\Delta_t = 0.027$ cm^{-1}	$\Delta_t = 0.049$ cm^{-1}
	$\tau_v = 5 \cdot 10^{-11}$ s	$\tau_v = 2.5 \cdot 10^{-11}$ s	$\tau_v = 1.5 \cdot 10^{-11}$ s	$\tau_v = 5.3 \cdot 10^{-11}$ s
$\Delta_t\tau_v = 1.0$				$D = 0.082$ cm^{-1}
	$\Delta_t = 0.05$ cm^{-1}	$\Delta_t = 0.028$ cm^{-1}	$\Delta_t = 0.020$ cm^{-1}	$\Delta_t = 0.049$ cm^{-1}
	$\tau_v = 10^{-10}$ s	$\tau_v = 3.1 \cdot 10^{-11}$ s	$\tau_v = 1.6 \cdot 10^{-11}$ s	$\tau_v = 1.0 \cdot 10^{-10}$ s

[a] Parameters in the slow-motion theory: $S = 7/2$, $\Delta_t = 0.05$ cm^{-1}, $D = 0$ or 0.1 cm^{-1}, and increasing values of τ_v.

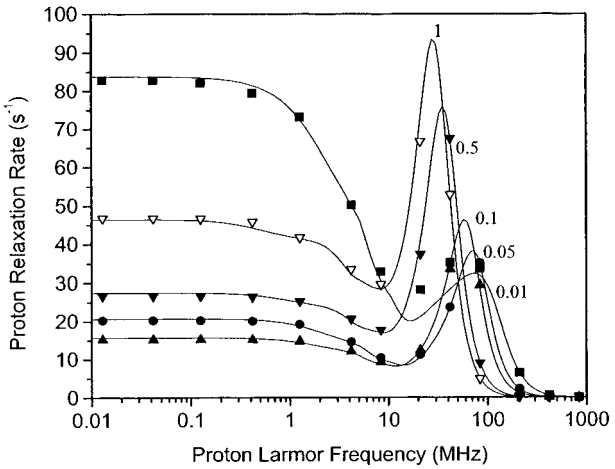

Figure 3. Proton relaxation rates calculated with the slow-motion theory ($\tau_v = 10^{-12}$ s, ■; 5×10^{-12} s, ●; 10^{-11} s, ▲; 5×10^{-11} s, ▼; 10^{-10} s, ▽) for $S = 7/2$ systems, two protons at 3.0 Å and $\Delta_t = 0.05$ cm^{-1}, $\tau_r = 10^{-6}$ s, $D = 0.1$ cm^{-1} and best fits (solid lines) performed using the modified Florence NMRD program of the profiles calculated with the slow-motion theory. The profiles are labeled with the value of $\Delta_t\tau_v$.

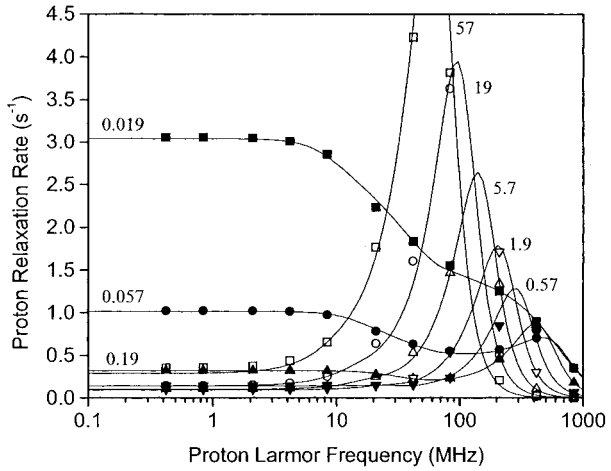

Figure 4. Proton relaxation rates calculated with the slow-motion theory ($\tau_v = 10^{-13}$ s, ■; 3×10^{-13} s, ●; 10^{-12} s, ▲; 3×10^{-12} s, ▼; 10^{-11} s, ▽; 3×10^{-11} s, △; 10^{-10} s, ○; 3×10^{-10} s, □) for $S = 1$ systems, two protons at 3.0 Å and $\Delta_t = 1$ cm^{-1}, $\tau_r = 10^{-6}$ s, $D = 1.2247$ cm^{-1} and best fits (solid lines) performed using the modified Florence NMRD program of the profiles calculated with the slow-motion theory. The profiles are labeled with the value of $\Delta_t\tau_v$.

We will now explain why the modified Florence model does not seem to be affected by the near-Redfield limit conditions and the reason for the increased difference in the low-field region between the slow-motion profiles and those of the SBM theory. The Redfield relaxation theory is based on perturbation theory. The perturbation theory assumes that the total Hamiltonian can be divided into the main, unperturbed part, which determines the gross energy-level features of the system, and into the perturbation part. The latter modifies the picture to a certain extent and, in the case of time-dependent perturbation, causes transitions between the energy levels. For stochastic perturbation, the transition probabilities are proportional to the spectral densities at frequencies corresponding to the energy differences between the (unperturbed) levels. If the product of the relevant interaction leading to the transitions/relaxation (here Δ_t) and the corresponding correlation time (here τ_v) is much smaller than unity, $\Delta_t\tau_v \ll 1$, the perturbation regime is always valid. When the Redfield conditions are approached, the inequality becomes less strong, the physical picture becomes dependent on the relative strengths of different interactions. If the magnetic field is low (the Zeeman interaction is weak) and the static ZFS is absent, the transient ZFS will tend to become the main Hamiltonian. The electron spin will then tend to be instantaneously quantized in the ZFS principal frame rather than in the laboratory frame. If $\Delta_t\tau_v \gg 1$, the electron spin will be completely locked in the transient ZFS frame and move with it. If τ_v is long, the motion of the electron spin will be slow, the correlation time sensed by the nuclear spin will be long, and the nuclear relaxivity will increase. Note that this picture is not valid at high field, where the Zeeman interaction acts as the unperturbed Hamiltonian, even if the Redfield condition is not fulfilled. The errors due to approaching the Redfield limit under these conditions are much less severe.

This explains the large differences in the low-field region between the slow-motion profiles and those of the SBM theory. In addition, it explains why the profiles of the slow-motion theory and the modified Florence model have different τ_v dependence than the SBM curves. The Bloembergen−Morgan equation (see eq 1) has a transition-frequency dependence that includes ω_S (i.e., the Zeeman frequency). At low magnetic fields, for all values of τ_v used in Figures 2−5, the product $\omega_S\tau_v$ in the denominator will always be less than unity, and thus, the electron spin relaxation rate will monotonically increase as τ_v increases (because $\Delta_t^2\tau_v$ increases), and in turn, the PRE

TABLE 4: Best-Fit Parameters Obtained Fitting the SBM Equations and the Modified Florence NMRD Program to the Slow-Motion Profiles Calculated without or with Static ZFS[a]

	values used in the slow motion calculation	best-fit parameters from the SBM theory	best-fit parameters from the modified Florence NMRD program
$\Delta_t\tau_v = 0.019$	$D = 1.2247\ cm^{-1}$		$D = 1.2\ cm^{-1}$
	$\Delta_t = 1\ cm^{-1}$	NO GOOD FITS	$\Delta_t = 1.0\ cm^{-1}$
	$\tau_v = 10^{-13}$ s		$\tau_v = 10^{-13}$ s
$\Delta_t\tau_v = 0.057$	$D = 1.2247\ cm^{-1}$		$D = 1.25\ cm^{-1}$
	$\Delta_t = 1\ cm^{-1}$	NO GOOD FITS	$\Delta_t = 1.0\ cm^{-1}$
	$\tau_v = 3\cdot10^{-13}$ s		$\tau_v = 3.0\cdot10^{-13}$ s
$\Delta_t\tau_v = 0.19$	$D = 1.2247\ cm^{-1}$		$D = 1.28\ cm^{-1}$
	$\Delta_t = 1\ cm^{-1}$	NO GOOD FITS	$\Delta_t = 0.98\ cm^{-1}$
	$\tau_v = 10^{-12}$ s		$\tau_v = 1.02\cdot10^{-12}$ s
$\Delta_t\tau_v = 0.57$	$D = 1.2247\ cm^{-1}$		$D = 1.29\ cm^{-1}$
	$\Delta_t = 1\ cm^{-1}$	NO GOOD FITS	$\Delta_t = 0.94\ cm^{-1}$
	$\tau_v = 3\cdot10^{-12}$ s		$\tau_v = 2.8\cdot10^{-12}$
$\Delta_t\tau_v = 1.9$	$D = 1.2247\ cm^{-1}$		$D \sim 1.2\ cm^{-1}$
	$\Delta_t = 1\ cm^{-1}$	$\Delta_t = 0.78\ cm^{-1}$	$\Delta_t = 0.77\ cm^{-1}$
	$\tau_v = 10^{-11}$ s	$\tau_v = 0.62\cdot10^{-11}$ s	$\tau_v = 0.64\cdot10^{-11}$ s
$\Delta_t\tau_v = 5.7$	$D = 1.2247\ cm^{-1}$		$D \sim 1.2\ cm^{-1}$
	$\Delta_t = 1\ cm^{-1}$	$\Delta_t = 0.62\ cm^{-1}$	$\Delta_t = 0.58\ cm^{-1}$
	$\tau_v = 3\cdot10^{-11}$ s	$\tau_v = 1.17\cdot10^{-11}$ s	$\tau_v = 1.12\cdot10^{-11}$ s
$\Delta_t\tau_v = 19$	$D = 1.2247\ cm^{-1}$		$D \sim 1.2\ cm^{-1}$
	$\Delta_t = 1\ cm^{-1}$	$\Delta_t = 0.43\ cm^{-1}$	$\Delta_t = 0.39\ cm^{-1}$
	$\tau_v = 10^{-10}$ s	$\tau_v = 0.19\cdot10^{-10}$ s	$\tau_v = 0.16\cdot10^{-10}$ s
$\Delta_t\tau_v = 57$	$D = 1.2247\ cm^{-1}$		$D \sim 1.2\ cm^{-1}$
	$\Delta_t = 1\ cm^{-1}$	$\Delta_t = 0.24\ cm^{-1}$	$\Delta_t = 0.23\ cm^{-1}$
	$\tau_v = 3\cdot10^{-10}$ s	$\tau_v = 0.24\cdot10^{-10}$ s	$\tau_v = 0.20\cdot10^{-10}$ s

[a] Parameters in the slow-motion theory: $S = 1$, $\Delta_t = 1\ cm^{-1}$, $D = 0$ or $1.2247\ cm^{-1}$, and increasing values of τ_v.

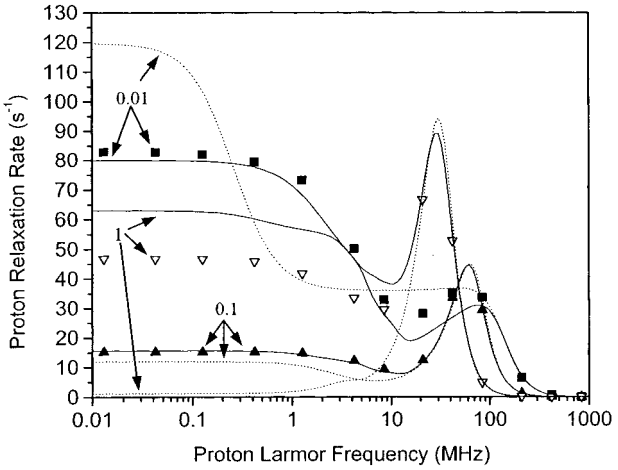

Figure 5. Proton relaxation rates calculated with the slow-motion theory ($\tau_v = 10^{-12}$ s, ■; 10^{-11}, ▲; p 10^{-10} s, ▽), with the modified Florence NMRD program (solid lines), and with the SBM equations (dotted lines) for $S = {}^7/_2$ systems, two protons at 3.0 Å and $\Delta_t = 0.05\ cm^{-1}$, $\tau_r = 10^{-6}$ s, $D = 0.12247\ cm^{-1}$. The profiles are labeled with the value of $\Delta_t\tau_v$.

decreases. On the other hand, if an axially symmetric static ZFS is present and the electron spin relaxation is within the Redfield limit, the static ZFS will be the main Hamiltonian at low field, and the electron spin will be quantized in the molecule-fixed static ZFS principal frame rather than in the laboratory frame. This means that the relevant frequencies, occurring in the spectral densities determining the electron spin relaxation in the low-field region, are related to the static ZFS rather than the Zeeman interaction. This feature is taken into account in the modified Florence model.[10] Indeed, instead of ω_S in the denominator of eq 1, we have ω_D. Because $\omega_D \gg \omega_S$ at low magnetic fields, the product $\omega_D\tau_v$ will be close to unity for $\tau_v = 50$ ps and $D = 0.1\ cm^{-1}$. This means that for $\tau_v < 50$ ps, $\omega_D\tau_v < 1$ and the electron spin relaxation depends on τ_v through $\Delta_t^2\tau_v$ analogously to eq 1. However, for $\tau_v > 50$ ps, $\omega_D\tau_v > 1$ and the electron spin relaxation rate becomes proportional to $1/\tau_v$ (i.e., $\Delta_t^2\tau_v/\omega_D^2\tau_v^2 \approx 1/\tau_v$), which leads to a reduction of the electron spin relaxation rate, and the increase of PRE, as τ_v increases.

The physical picture of the electron spin relaxation in the slow-motion regime is dependent on the relative magnitudes of the transient and static ZFS. If the magnitude of the transient ZFS is comparable to that of the static part of the ZFS, the same feature as without static ZFS will be present. Thus, the electron spin will instantaneously be quantized, at least partly, in the transient rather than in the static ZFS principal frame, and the energy-level structure will then be influenced also by the transient ZFS.

If, on the other hand, the static ZFS is larger than the transient, then the general shape of the spectral density functions determining the electron spin relaxation in the low-field region is related to the static ZFS, which reduces the sensitivity to fulfilling the condition $\Delta_t\tau_v \ll 1$. Thus, the good agreement in the low-field region between the slow-motion calculations and the modified Florence NMRD profiles is caused by the fact that the magnitude of the static ZFS is about twice that of the transient ZFS.

Conclusions

The aim of the present paper is the understanding of the physics of electron spin relaxation near the Redfield limit. To do that, we compare different models comprising different levels of sophistication.

The SBM equations can provide reasonably good fits of experimental relaxometric profiles if static ZFS is absent. The obtained best-fit parameters may, however, be subject to large errors if the electron spin relaxation is close to or out of the Redfield limit, which seems to be the case of the commonly employed and investigated Gd-based contrast agents. The SBM theory does not take into account the static ZFS; this fact can produce even larger errors in the obtained parameter values. A notable result of the calculations in the present paper is that, by approaching the Redfield limit, the $\Delta_t\tau_v$ product is always

smaller when experimental profiles are fitted with the SBM theory, than with the slow-motion theory. The reason is that the former theory predicts a smaller low-field plateau than the latter, which is a consequence of the poor description of the electron spin relaxation near the Redfield limit in the SBM theory. Thus, the comparisons in the present paper indicate that when experimental profiles of Gd-based contrast agents are fitted with the SBM equations, the obtained best-fit values of Δ_t and τ_v are clearly underestimated (several tens of percent smaller than the correct values). The difference becomes even larger if a static ZFS is present.

The modified Florence model produces very good fits with obtained best-fit parameter values that are in good agreement with those used in the slow-motion calculations, even under near-Redfield limit conditions. This is likely to hold as long as the magnitude of the static ZFS is larger than that of the transient ZFS. This shows that systems with static ZFS near the Redfield limit can still be described with the Redfield approach if the correct energy level effects are included in the electron spin relaxation. This is important because it validates analysis of the experimental data using the proper approximations.

Such considerations can be important for future development of contrast agents for MRI. In fact, last-generation contrast agents are developed in order to have a value for the exchange time of water protons coordinated to the metal ion of the same order of the electron spin relaxation time at the fields of work of MRI.[17] Therefore, calculations done with the SBM equation to optimize the value of τ_M can be significantly affected by the closeness of the Redfield limit for electron spin relaxation. Furthermore, the present findings are crucial for the development of contrast agents to be used at low fields, where the values of relaxivity calculated with the SBM equations can be profoundly incorrect. Consequently, the modified Florence model or an equivalent approach should preferably be used rather than the SBM theory under near-Redfield limit conditions for cases when the static part is larger than the transient part of the ZFS, which is likely to occur in, e.g., Gd-based contrast agents.

Acknowledgment. We are grateful to Dr Danuta Kruk for valuable discussions. Generous grants of computer time by the Center for Parallel Computers in Stockholm are gratefully acknowledged. This work has been supported by Murst ex 40%, Italy, the European Union (Contract HPRI-CT-1999-00009, Contract HPRN-CT-2000-00092, Contract HPRI-CT-2001-50028 and Contract BIO4-CT98-0156), CNR, Progetto Finalizzato Biotecnologie, Italy (Contract 990039349), CNR Commitato nazionale per le scienze chimiche, Italy (Contract 970113349), and the Swedish Natural Science Research Council.

References and Notes

(1) Banci, L.; Bertini, I.; Luchinat, C. Nuclear and electron relaxation. *The magnetic nucleus-unpaired electron coupling in solution*; VCH: Weinheim, Germany, 1991.

(2) Kowalewski, J. *Encyclopedia of Nuclear Magnetic Resonance*; Wiley: Chichester, U.K., 1996.

(3) Bertini, I.; Luchinat, C.; Parigi, G. *Solution NMR of Paramagnetic Molecules*; Elsevier: Amsterdam, The Netherlands, 2001.

(4) Solomon, I. *Phys. Rev.* **1955**, *99*, 559.

(5) Bloembergen, N. *J. Chem. Phys.* **1957**, *27*, 575.

(6) Bloembergen, N.; Morgan, L. O. *J. Chem. Phys.* **1961**, *34*, 842.

(7) Bertini, I.; Galas, O.; Luchinat, C.; Parigi, G. *J. Magn. Reson. Ser. A* **1995**, *113*, 151.

(8) Sharp, R. R. *J. Chem. Phys.* **1993**, *98*, 912.

(9) Bertini, I.; Kowalewski, J.; Luchinat, C.; Nilsson, T.; Parigi, G. *J. Chem. Phys.* **1999**, *111*, 5795.

(10) Kruk, D.; Nilsson, T.; Kowalewski, J. *Phys. Chem. Chem. Phys.* **2001**, *3*, 4907.

(11) Koenig, S. H.; Brown, R. D., III. *Prog. NMR Spectrosc.* **1990**, *22*, 487.

(12) Uggeri, F.; Aime, S.; Anelli, P. L.; Botta, M.; Brocchetta, M.; De Haen, C.; Ermondi, G.; Grandi, M.; Paoli, P. *Inorg. Chem.* **1995**, *34*, 633.

(13) Elst, L. V.; Maton, F.; Laurent, S.; Seghi, F.; Chapelle, F.; Muller, R. N. *Magn. Res. Med.* **1997**, *38*, 604.

(14) Bertini, I.; Luchinat, C.; Parigi, G.; Quacquarini, G.; Marzola, P.; Cavagna, F. M. *Magn. Res. Med.* **1998**, *39*, 124.

(15) Toth, E.; Connac, F.; Helm, L.; Adzamli, K.; Merbach, A. *Eur. J. Inorg. Chem.* **1998**, 2017.

(16) Aime, S.; Botta, M.; Fasano, M.; Terreno, E. *Chem. Soc. Rev.* **1998**, *27*, 19.

(17) Caravan, P.; Ellison, J. J.; McMurry, T. J.; Lauffer, R. B. *Chem. Rev.* **1999**, *99*, 2293.

(18) Bligh, S. W. A.; Chowdhury, A. H. M. S.; Kennedy, D.; Luchinat, C.; Parigi, G. *Magn. Res. Med.* **1999**, *41*, 767.

(19) Anelli, P. L.; Bertini, I.; Fragai, M.; Lattuada, L.; Luchinat, C.; Parigi, G. *Eur. J. Inorg. Chem.* **2000**, 625.

(20) Botta, M. *Eur. J. Inorg. Chem.* **2000**, *3*, 399.

(21) Bertini, I.; Luchinat, C. *NMR of paramagnetic molecules in biological systems*; Benjamin/Cummings: Menlo Park, CA, 1986.

(22) Bertini, I.; Galas, O.; Luchinat, C.; Messori, L.; Parigi, G. *J. Phys. Chem.* **1995**, *99*, 14217.

(23) Bertini, I.; Luchinat, C.; Mincione, G.; Parigi, G.; Gassner, G. T.; Ballou, D. P. *JBIC* **1996**, *1*, 468.

(24) Kroes, S. J.; Salgado, J.; Parigi, G.; Luchinat, C.; Canters, G. W. *JBIC* **1996**, *1*, 551.

(25) Powell, D. H.; Dhubhghaill, O. M. N.; Pubanz, D.; Helm, L.; Lebedev, Y. S.; Schlaepfer, W.; Merbach, A. E. *J. Am. Chem. Soc.* **1996**, *118*, 9333.

(26) Rast, S.; Borel, A.; Helm, L.; Belorizky, E.; Fries, P. H.; Merbach, A. E. *J. Am. Chem. Soc.* **2001**, *123*, 2637.

(27) Larsson, T.; Westlund, P. O.; Kowalewski, J.; Koenig, S. H. *J. Chem. Phys.* **1994**, *101*, 1116.

(28) Svoboda, J.; Nilsson, T.; Kowalewski, J.; Westlund, P. O.; Larsson, P. T. *J. Magn. Reson. Ser. A* **1996**, *121*, 108.

(29) Benetis, N.; Kowalewski, J.; Nordenskiöld, L.; Wennerström, H.; Westlund, P. O. *Mol. Phys.* **1983**, *50*, 515.

(30) Benetis, N.; Kowalewski, J.; Nordenskiöld, L.; Wennerström, H.; Westlund, P. O. *Mol. Phys.* **1983**, *48*, 2.

(31) Kowalewski, J.; Nordenskiöld, L.; Benetis, N.; Westlund, P. O. *Prog. NMR Spectrosc.* **1985**, *17*, 141.

(32) Rubinstein, M.; Baram, A.; Luz, Z. *Mol. Phys.* **1971**, *20*, 67.

(33) Abernathy, S. M.; Sharp, R. R. *J. Chem. Phys.* **1997**, *106*, 9032.

(34) Geraldes, C. F.; Brown, R. D., III.; Brucher, E.; Koenig, S. H.; Sherry, A. D.; Spiller, M. *Magn. Reson. Med.* **1992**, *27*, 284.

(35) Strandberg, E.; Westlund, P. O. *J. Magn. Reson. Ser. A* **1996**, *122*, 179.

(36) Borel, A.; Yerly, F.; Helm, L.; Merbach, A. E. *J. Am. Chem. Soc.* **2002**, *124*, 2042.

(37) Nilsson, T.; Parigi, G.; Kowalewski, J. *J. Phys. Chem. A* **2002**, *106*, 4476.

(38) Nilsson, T.; Kowalewski, J. *Mol. Phys.* **2000**, *98*, 1617; erratum: *Mol. Phys.* **2001**, *99*, 369.